HHS Public Access

Author manuscript

Oncogene. Author manuscript; available in PMC 2010 September 25.

Published in final edited form as:

Oncogene. 2010 March 25; 29(12): 1720–1731. doi:10.1038/onc.2009.465.

Defective DNA double-strand break repair underlies enhanced tumorigenesis and chromosomal instability in p27 deficient mice with growth-factor induced oligodendrogliomas

Wendy L. See[1], **Jeffrey P. Miller**[2], **Massimo Squatrito**[3], **Eric Holland**[3], **Marilyn D. Resh**[1,*], and **Andrew Koff**[2,*]

[1] Programs in Cell Biology, Memorial Sloan-Kettering Cancer Center, New York, NY 10065

[2] Molecular Biology, Memorial Sloan-Kettering Cancer Center, New York, NY 10065

[3] Cancer Biology & Genetics, Memorial Sloan-Kettering Cancer Center, New York, NY 10065

Abstract

The tumor suppressive activities of the Kip-family of cdk inhibitors often go beyond their role in regulating the cell cycle. Here, we demonstrate that p27 enhances Rad51 accumulation during repair of double-strand DNA breaks. Progression of PDGF-induced oligodendrogliomas was accelerated in mice lacking the cyclin-cdk binding activities of $p27^{kip1}$. Cell lines were developed from RCAS-PDGF infection of nestin-tv-a brain progenitor cells in culture. p27 deficiency did not affect cell proliferation in early passage cell lines; however, the absence of p27 affected chromosomal stability. In p27 deficient cells, the activation of Atm and Chk2, and the accumulation of γH2AX was unaffected compared to wild type cells, and the number of phospho-histone H3 staining mitotic cells was decreased, consistent with a robust G2/M checkpoint activation. However, the percentage of Rad51 foci positive cells was decreased, and the kinase activity that targets the C-terminus of BRCA2, regulating BRCA2/Rad51 interactions, was increased in lysates derived from p27 deficient cells. Increased numbers of chromatid breaks in p27 deficient cells that adapted to the checkpoint were also observed. These findings suggest that Rad51-dependent repair of double stranded breaks was hindered in p27 deficient cells, leading to chromosomal instability, a hallmark of cancers with poor prognosis.

Keywords

p27; tumor suppressor; DNA repair; glioma; mouse model

Introduction

Gliomas are the most common adult brain neoplasm, and are divided into astrocytomas, oligodendrogliomas (ODGs), mixed gliomas, and glioblastoma multiforme. Normal glial

* Corresponding Authors Memorial Sloan-Kettering Cancer Center 1275 York Avenue, Box 207 New York, NY 10065 Phone: 212-639-2354; FAX: 646-422-2062 a-koff@ski.mskcc.org, m-resh@ski.mskcc.org.

cell development and formation of glial tumors are both regulated by PDGF signaling. PDGF is often co-expressed with the PDGF receptor in human gliomas, including ODGs (Di Rocco et al., 1998; Shih et al., 2004), and retroviral expression of PDGF induces ODG formation in mouse models (Dai et al., 2001). Treatment with PDGF receptor kinase inhibitors blocks the growth of these gliomas in mice (Shih et al., 2004; Uhrbom et al., 1998).

PDGF signaling plays a crucial role in gliomagenesis, but the influence of PDGF activation on downstream events in glial tumor cells is poorly understood. We hypothesized that alterations in cell cycle regulators might contribute to the development of ODG. Cell cycle progression is driven by the activity of cyclin dependent kinases (cdk). If cdk activity drops below a threshold, the cell withdraws from the cell cycle. Two families of cdk inhibitors (cki) negatively regulate the activities of the cdks. The Ink4a family (p15, p16, p18, p19) inhibits cyclin D-cdk4/6 complexes while the Cip/Kip subfamily (p21, p27, p57) inhibits cyclin-cdk2 complexes (Sherr and Roberts, 1995; Sherr and Roberts, 1999).

One cki, $p27^{Kip1}$, may be especially important in ODG. Oligodendrocyte progenitor cells (OPCs) are one of the precursor cell-types in which ODG develops. Differentiation of OPCs in response to PDGF withdrawal depends on the timely accumulation of p27 (Casaccia-Bonnefil et al., 1997; Durand et al., 1998). PTK787, a compound that blocks PDGF signaling, induces differentiation of PDGF-transformed glial progenitors into oligodendrocytes and accumulation of p27 (Dai et al., 2001). Decreased p27 protein expression is associated with decreased survival in human ODG (Cavalla et al., 1999; Kamiya and Nakazato, 2002; Korshunov et al., 2002). Thus, p27 deficiency might contribute to ODG by maintaining the tumor progenitor cell in a proliferative state.

In human ODG, p27 protein levels do not correlate with proliferation (Cavalla et al., 1999), suggesting that changes in p27 expression may be unrelated to its ability to control cell cycle exit. Tumor progression induced by a variety of challenges (carcinogens, oncogenes, or tumor suppressor loss), is accelerated in p27 deficient mice (Blain et al., 2003; Cipriano et al., 2001; Di Cristofano et al., 2001; Fero et al., 1998; Koff, 2006; Martins and Berns, 2002; Musgrove et al., 2004; Park et al., 1999; Shaffer et al., 2005). Accelerated progression is sometimes associated with increased proliferation indices, and other times it is not. Thus, we began these studies to better define the effect of p27 deficiency in ODG.

Here, we used the RCAS/tv-a system to generate PDGF-induced ODG in mice (Uhrbom and Holland, 2001). The avian retrovirus RCAS cannot infect mammalian cells. However, mice that are transgenic for the tv-a receptor under the nestin promoter (Ntv-a) allow tissue specific infection of OPC and other earlier neuronal/glial cell types (Doetsch et al., 1997; Doetsch et al., 2002; Holland, 2001). We crossed Ntv-a transgenic mice onto a p27 deficient ($p27^{D51/D51}$) background. The D51 p27 allele is missing the first 51 amino acids of p27; this mutant protein does not bind cyclin-cdk complexes (Kiyokawa et al., 1996). $p27^{D51/D51}$ homozygous mice and cells derived from these mice have phenotypes similar to other p27 null animals (Fero et al., 1996; Nakayama et al., 1996).

Our results show that p27 deficiency enhances tumor progression and leads to a dramatic decrease in survival in PDGF-induced oligodendrogliomas. We also established PDGF-transformed glial cultures. Early passage p27 deficient PDGF-infected glial cells grew at the same rate as wild type controls, but contained a number of chromosomal abnormalities, indicating that they suffered from genomic instability. In response to γ-irradiation, more chromatid breaks and a decrease in the formation of Rad51 repair foci were observed in p27 deficient cells. Activation of Atm, and Chk2, and accumulation of γH2AX were equivalent. Together this suggested that p27 deficiency attenuated DNA repair in G2 cells. We propose that the absence of p27 may create a permissive environment in which chromosomal abnormalities that lead to enhanced proliferation can be selected for in the tumor environment.

Results

PDGF-induced ODG progresses more rapidly in p27 deficient mice

p27 acts as a tumor suppressor in several mouse models of cancer (Blain et al., 2003; Cipriano et al., 2001; Di Cristofano et al., 2001; Fero et al., 1998; Martins and Berns, 2002; Park et al., 1999; Shaffer et al., 2005). Loss of p27 expression correlates with decreased survival in human ODG (Cavalla et al., 1999; Kamiya and Nakazato, 2002; Korshunov et al., 2002), suggesting that p27 might play a contributing role in ODG. To determine if loss of p27 had an effect on PDGF-driven gliomagenesis, we crossed nestin-tva (Ntv-a) mice onto a p27 mutant ($p27^{D51/\Delta 51}$) background. The protein produced by this allele lacks the amino terminal 51 amino acids and does not bind cyclin-cdk complexes. Tumor formation was induced with the RCAS/tv-a system. HA tagged PDGF was sub-cloned into the RCAS vector (RCAS-PDGF-HA) (Shih et al., 2004) to promote constitutive expression of PDGF. Chicken DF1 cells were transfected with RCAS-PDGF-HA, and virus-producing cells were directly injected into the frontal cortex of newborn pups to allow for viral infection of proliferating cells in the subventricular zone. We used transgenic mice that express the tv-a receptor under the nestin promoter, which restricts infection to neural/glial progenitors, glial restricted progenitors, OPC and astrocyte precursors.

$p27^{+/+}$, $p27^{+/D51}$, and $p27^{D51/D51}$ mice were injected with 10^4 DF1 cells that produced the RCAS-PDGF-HA virus and evaluated for 12 weeks. Mice were sacrificed earlier if they became morbid. Virtually all tv-a negative mice, regardless of their p27 genotype, were still alive at the end of 12 weeks, and as expected, none had any evidence of tumor when sacrificed. Thus the following descriptions focus solely on those mice that express tv-a. The onset of morbidity was equivalent in the $p27^{D51/D51}$ and $p27^{D51/+}$ animals, with 50% having to be sacrificed by the fourth week compared to nine weeks for $p27^{+/+}$ mice (Figure 1A). H&E staining demonstrated that >95% of the mice sacrificed had a tumor. Tumors were diffuse and consisted of small cells; there was evidence of perivascular and perineuronal satellitosis, white matter tracking, and subpial infiltration (Liu et al., 2007). At the end of 12 weeks, only 6% of $p27^{D51/D51}$ mice and 20% of $p27^{+/D51}$ mice remained alive compared to 38% of the $p27^{+/+}$ mice. Virtually all the mice that survived to 12 weeks had tumors. The differences in survival were statistically significant by log-rank analysis. Thus, genetic

deficiency of p27, either at one or both alleles, was sufficient to increase morbidity and mortality associated with enforced expression of PDGF.

To determine if p27 deficiency affected the nature of the disease, three tumors from $p27^{+/+}$ and $p27^{D51/D51}$ animals were randomly selected for further analysis by immunohistochemistry. Both the $p27^{+/+}$ and $p27^{D51/D51}$ tumors were positive for the oligodendrocyte marker olig2 (Liu et al., 2007) and the stem cell marker sox2 (Avilion et al., 2003; Ferri et al., 2004) (Figure 1B), and negative for the neuronal marker NeuN (Jin et al., 2003). With the exception of trapped astrocytes, the tumors were also negative for GFAP. Thus, the presence of two p27 alleles contributed to better prognosis and longer survival when ODG was driven by expression of the growth factor PDGF.

p27 is a haploinsufficient tumor suppressor that is not dose-dependent in PDGF-induced ODG

In most other tumor models, haploinsufficiency at the p27 locus manifests as dosage-dependence—heterozygous mice succumb to disease at a rate intermediate to that observed in wild type or nullizygous mice (Fero et al., 1998; Park et al., 1999). However, in PDGF-induced ODG, symptom free survival was equivalent for $p27^{+/D51}$ mice and $p27^{D51/D51}$ animals ($P<0.5$, Figure 1A), suggesting that in this tumor type p27 might not be dose-dependent. We determined whether p27 protein was still produced by the wild-type allele. Nuclear expression of p27 was observed in both $p27^{+/+}$ and $p27^{+/D51}$ tumors, but not in the $p27^{D51/D51}$ tumors (Figure 1C). Thus the tumor suppressive effect of p27 is not dosage dependent in this tumor type.

p27 deficiency does not affect PDGF expression from RCAS vectors, alter PDGF signaling pathways, or increase proliferation in incipient tumor cells

It was formally possible that p27 loss exerted its effects in this system by altering PDGF signaling. Unlike many solid tumors, ODG are diffuse and contain highly motile cells. The masses are heterogeneous and contain both oligodendrocyte tumor cells and uninfected oligodendrocytes, making direct measurement of proliferation or apoptotic indices on tumor cells problematic. We therefore employed an approach that allows us to overcome these limitations. We previously demonstrated that cell lines can be developed that recapitulate the molecular and cellular features of incipient tumor cells (Dai et al., 2001; Liu et al., 2007; Soos et al., 1996). Post-natal day 1 Ntv-a positive $p27^{+/+}$ or $p27^{D51/D51}$ brains were cultured for 4 days and infected with an RCAS virus that expresses PDGF-HA under control of the viral LTR and GFP under the control of the SV40 promoter (Becher et al., 2008). Following infection and passaging for 6 weeks, we generated wild type (WT1) and p27 deficient (KO1) cultures in which greater than 99% of the cells expressed GFP (Figure 2A, upper panels). RCAS integration was confirmed by fluorescence in situ hybridization (Figure 2A, lower panels).

Western blotting revealed that both WT1 and KO1 PDGF-infected glial cell lines evaluated at early passage (≤p20) expressed equal amounts of HA-tagged PDGF and activated phospho-PDGFRβ (Figure 2B, compare lanes 1 and 3). Levels of phospho-Erk1/2 (pERK1/2), phospho-p70S6kinase (pp70S6K) and cyclin D1 were similar between the

genotypes, but there was a modest increase in the expression of p21 and cyclin A in the KO1 cells (Figure 2B, compare lanes 1 and 3). When cells were treated with the receptor tyrosine kinase inhibitor PTK787, levels of pERK1/2, pp70S6K, and cyclin D1 were decreased to similar extents in both WT1 and KO1 cells. Levels of Rad51, a protein involved in DNA repair, were equivalent. Although the amount of PDGFR phosphorylation, cyclin A and p21 also decreased in the KO1 cells relative to controls, the decreases were not as strong as those observed in the WT1 cells (Figure 2B, compare lanes 2 and 4). Nevertheless, treatment reduced DNA replication as measured by BrdU incorporation in both WT1 and KO1 cells (Figure 3B). There was a trend towards PTK787 resistance in the p27 deficient culture, although this was not statistically significant, and apoptosis was equivalent in WT1 and KO1 cells in the presence or absence of PTK787 (data not shown). Thus, p27 deficiency did not appear to grossly alter PDGF signaling, or the requirement of PDGF for proliferation.

In early passage cell populations, the growth and proliferation rates of the $p27^{+/+}$ and $p27^{D51/D51}$ PDGF- infected glial cultures were equivalent (Figure 3A and B). As passage number increased, the p27 deficient cells exhibited an accelerated growth rate (Figure 3C) and increased proliferation, based on BrdU incorporation ($P<0.02$) (Figure 3D) compared to the wild type cells. Apoptotic indices, measured either by FACS analysis of Annexin V staining or immunoblot analysis of cleaved caspase 3, were unaffected (data not shown). These data suggest that loss of p27 did not affect the early growth response to the oncogenic signal, but that over time p27 deficiency was associated with the evolution of a more proliferative cell type.

Karyotypic abnormalities are more frequent in p27 deficient PDGF-infected glial cell lines

One non-cell cycle related mechanism by which p27 deficiency might contribute to tumor development is to increase genomic instability (Chibazakura et al., 2004; Payne et al., 2008; Shaffer et al., 2005; Spruck et al., 1999; Strohmaier et al., 2001)g. We therefore addressed whether there was an increase in genomic instability during the early neoplastic changes occurring in PDGF-expressing glial cells. An additional set of independently derived wild type (WT2) and p27 deficient (KO2) cultures was established. More p27 deficient cells had an abnormal karyotype in early passage cultures (KO1 and KO2), compared to early passage wild type cultures (WT1 and WT2) (Table 1). The few abnormal karyotypes observed in the WT1 and WT2 cultures consisted of aneuploid and tetraploid cells. By contrast, many of the abnormalities observed in p27 deficient cultures also included translocations, segmental duplications and inversions (data not shown and Table 1). A few representative karyotypes of normal cells and abnormal cells are shown in Supplementary Figure 1. We attempted to culture primary brain tumors from tumor bearing mice for karyotype analysis. Only 1 of 5 primary tumors from $p27^{+/+}$ mice proliferated in tissue culture whereas 2/2 $p27^{D51/D51}$ tumors proliferated well in culture. Thus, we were only able to analyze one set of age matched $p27^{+/+}$ and $p27^{D51/D51}$ tumor cultures. The $p27^{D51/D51}$ cells had an increased number of abnormal cells compared to $p27^{+/+}$ cells that was statistically significant (Table 1). The increased number of abnormalities suggests that the degree of chromosomal instability is elevated in p27 deficient cells, or that the mechanisms that eliminate such cells from the culture are incapacitated in p27 deficient cells.

p27 deficiency does not diminish the G2/M checkpoint invoked by the DNA damage response

Increased genomic instability in tumor cells might occur as a consequence of defects in DNA repair or checkpoint fidelity. To evaluate these possibilities, we irradiated early passage cells to induce DNA double strand breaks and evaluated three proteins involved the DNA damage response: Atm, Chk2, and γH2AX. Thirty minutes after γ-irradiation, levels of phospho-ATM, the activated form of ATM kinase, increased in both WT1 and KO1 cells (Figure 4A) and returned to near basal levels by three hours. Chk2 phosphorylation was maximally increased by 30 minutes following irradiation, and increased levels were maintained over the duration of the experiment. γH2AX, a marker of DNA double strand breaks (Foster and Downs, 2005), also increased in both wild type and p27 deficient cells by 30 minutes following IR. We did not observe a significant difference in γH2AX accumulation between wild type and p27 deficient cells before or after irradiation (Figure 4A and data not shown). Similar results were observed in WT2 and KO2 cells (data not shown). Together, these results suggest that activation of the DNA damage response, at least in response to ionizing radiation, was largely equivalent in the wild type and p27 deficient cells.

We next looked downstream to G2/M checkpoint activation in response to γ-irradiation (Figure 4B). Phospho-histone H3 is a convenient flow cytometric marker for mitotic cells. Cells with unrepaired DNA double-strand breaks arrest prior to mitosis and are negative for phospho-histone H3. When WT1 cells were exposed to either 1 or 2 Gy, the number of mitotic cells decreased approximately 47% or 70%, respectively, compared to unirradiated controls. In KO1 cells, the number of mitotic cells decreased 66% and 88%. Pretreatment with caffeine, an inhibitor of ATM kinase activity (Sarkaria et al., 1999), abrogated G2/M checkpoint activation in both WT1 and KO1 cells (Figure 4B). Similar results were obtained with WT2 and KO2 cells (data not shown). Thus p27 deficient cells appear capable of pausing at the G2/M checkpoint to repair DNA damage. To determine if G2/M checkpoint activation was intact *in vivo*, we irradiated tumor bearing mice (10 Gy), and performed phospho-histone H3 immunohistochemistry three hours after irradiation. We also analyzed tumors from unirradiated control mice. The percent of phospho-histone H3 positive cells was similar between $p27^{+/+}$ and $p27^{D51/D51}$ unirradiated tumors (Figure 4C and D). No phospho-histone H3 positive cells were identified in either $p27^{+/+}$ or $p27^{D51/D51}$ tumors three hours after irradiation. We also looked at the induction of apoptosis. Similar amounts of cleaved caspase 3 and TUNEL staining were seen at 3 and 12 hours, respectively, in wild type and mutant animals (data not shown). These results confirm that G2/M checkpoint activation was intact *in vivo*.

p27 deficiency affects the persistence of Rad51 foci formed and phosphorylation of the C-terminus of BRCA2 in response to DNA damage

DNA double strand breaks are repaired by either Rad51 mediated homologous recombination or non-homologous end joining (NHEJ). p27 deficient cells display reciprocal translocations, implying that NHEJ is intact (Weinstock et al., 2006). Since homologous recombination has been proposed to be the main DNA repair pathway utilized

by cancer cells (Powell and Bindra, 2009) and is favored in cells in G2, we focused our attention on homologous recombination.

We irradiated early passage wild type and p27 deficient cells and scored Rad51 foci over the next 24 hours. Formation of Rad51 nuclear foci is a quantitative measure of DNA repair by homologous recombination (Haaf et al., 1995; Raderschall et al., 1999). Since normal S-phase cells may contain up to five such foci, we required that a cell have greater than five foci to score positive. The percentage of wild type and p27 deficient cells containing Rad51 nuclear foci was similar one hour after irradition (Figure 5B), but there was a significant difference at three hours. Fewer KO1 cells (34%) formed Rad51 foci compared to WT1 cells, (62%) (*$P<0.001$) (Figure 5A and B). Similar results were obtained in WT2 and KO2 cells (data not shown). By 24 hours, WT1 cells had basal levels of Rad51 foci positive cells. However, more KO1 cells contained Rad51 foci, 11% compared to 3% of WT1 cells (**$P<0.05$) (Figure 5B), suggesting that p27 deficient cells were unable to repair double strand breaks as efficiently as wild type cells.

The measurement of Rad51 foci positive cells could reflect differences in Rad51 protein levels or in the distribution of cells in various phases of the cell cycle. However, Rad51 protein levels and propidium iodide stained flow cytometric profiles of WT1 and KO1 cells were comparable at all time points (Figure 5C and D). Levels of Mre11 and Ku70, proteins involved in sensing DNA damage and NHEJ, respectively, were equivalent before and after irradiation in both wild type and p27 deficient cells (Figure 5C). These results indicate that the accumulation or maintenance of Rad51 nuclear foci in response to irradiation was perturbed in p27 deficient cells, suggesting that p27 contributes to homologous recombination-dependent DNA repair mechanisms.

The efficiency of homologous recombination can be modulated by cdk activity (Aylon et al., 2004; Esashi et al., 2005; Huertas et al., 2008). Cdk-mediated phosphorylation of Ser3291 within the C-terminus of BRCA2 blocks BRCA2/Rad51 interactions and prevents Rad51-mediated DNA repair (Esashi et al., 2005). Since loss of p27 may lead to enhanced cdk activity, we monitored cdk activity in p27 deficient cells using TR2, a C-terminal BRCA2 peptide containing Ser3291, as a substrate. WT1 and KO1 cells were irradiated (5 Gy) and lysed at 0, 1, 2, 3, or 4 hours post-irradiation. Lysates were incubated with GST or GST-TR2 bound to Sepharose beads and labeled with [γ-^{32}P]ATP (Figure 5E). Phosphorylation of TR2 decreased by 50% one hour after irradiation in WT1 cells (black bars) and increased back to basal levels by 3 hours (Figure 5F). By contrast, phosphorylation of TR2 remained unchanged in KO1 cells (open bars) at all time points, suggesting that p27 deficient cells contained elevated GST-TR2 phosphorylation activity after exposure to γ-irradiation.

To determine if cdk activity was altered in p27 deficient cells, kinase assays were performed using Histone H1 as a substrate. Cyclin B1-associated kinase activity was reduced after irradiation in WT1 cells (Supplementary Figure 2A, black bars). However, there was a more modest decrease in KO1 cells (Supplementary Figure 2A, open bars), suggesting that cyclin B1-associated kinase activity could be partially mediating the BRCA2-TR2 phosphorylation activity in p27 deficient cells. Cdk2 kinase activity decreased in WT1 cells (Supplementary Figure 2B, black bars) after irradiation with an even longer response observed in KO1 cells

(Supplementary Figure 2B, open bars). These results demonstrate that p27 deficient cells are responsive to DNA damage inducing checkpoints and suggest that elevated kinase activity associated with p27 deficiency following ionizing radiation may perturb the function of BRCA2.

The frequency of chromatid breaks is increased in p27 deficient cells

Cells that fail to repair DNA double-strand breaks during the G2/M checkpoint either die, or "adapt" to the checkpoint by progressing into mitosis with chromatid breaks. To determine if p27 deficiency increased the number of chromatid breaks in mitotic cells, wild type and p27 deficient cells were irradiated with 1 Gy, and allowed to recover for 1.5 hours prior to the addition of colcemid. No chromosome breaks/gaps or chromatid breaks were observed in unirradiated WT1, WT2, KO1, or KO2 cells (data not shown). We therefore focused our analysis on the presence of chromatid breaks, an indicator of repair defects in G2 when homologous recombination occurs. There were two-fold more mitotic cells with greater than three chromatid breaks in KO1 cultures compared to WT1 cultures (P=0.02) (Figure 6A), and seven-fold more mitotic cells with greater than three breaks in KO2 cells compared to WT2 cells (P<0.01) (data not shown) There was a higher incidence of Rad51 foci in p27 deficient cells at 24 HR post-irradiation (Figure 5B). To determine if this correlated with an increase in unrepaired breaks, we irradiated WT1 and KO1 cells with 5 Gy and analyzed 100 metaphases 24 HR after irradiation. There was an increase in the number of mitotic cells containing unrepaired breaks, 12% in KO1 versus 4% in WT1 (P=0.03) (Figure 6B). When metaphase spreads were prepared from unirradiated primary tumor cultures, we observed more mitotic cells with unrepaired breaks in the $p27^{D51/D51}$ primary tumor culture compared to the age matched $p27^{+/+}$ primary tumor culture (P<0.02) (Table 2). These findings suggest that p27 deficient cells were less proficient at repairing DNA double strand breaks in G2 and eventually progressed to mitosis with broken chromatids. Thus, loss of p27 diminishes the cell's ability to repair DNA double strand breaks, leading to chromosomal instability, a hallmark of cancers with poor prognosis.

Discussion

The purpose of this study was to examine the contribution of p27-mediated tumor suppression in PDGF-driven ODGs. We show that p27 deficiency dramatically alters survival and tumor progression. We developed a tissue culture model of PDGF-driven glial tumorigenesis and found that p27 deficiency affects chromosomal stability and DNA repair at a time when there were no effects on proliferation. Our results thus uncover a cell cycle-independent function for p27 that regulates genome stability in ODGs.

p27 deficiency leads to genomic instability, independent of its role in cellular proliferation

It is now well accepted that p27 loss is an indicator of poor prognosis for a variety of human neoplasms. The tumor suppressive role of p27 has been validated in a number of mouse models. In some human tumors and mouse models, p27 loss correlates with increased proliferation (Blain et al., 2003; Koff, 2006), whereas in others p27 loss does not (Carneiro et al., 2003; Porter et al., 1997; Shaffer et al., 2005). It is not understood what type of

contribution p27 deficiency makes to tumor progression in those circumstances where it appears to be independent of the cell cycle.

p27 is an inhibitor of cdk activity and uncontrolled cdk activity can contribute to genetic instability (Chibazakura et al., 2004; Spruck et al., 1999; Strohmaier et al., 2001). Precisely how cdk activity leads to genetic instability is still unresolved in tumors. It has been difficult to develop models that validate the relationship between loss of p27 and defects in genomic integrity. The results presented here clearly demonstrate that p27 deficiency accelerates the rate of tumor progression and morbidity associated with PDGF-driven ODG independently of a cell cycle effect. Regardless of p27 genotype, the incipient PDGF-expressing tumor cells, analyzed in vitro, behave similarly with respect to proliferation, cytokine dependence and signaling. It is only after continued passage that p27 deficient cultures evolve into a more proliferative collection of cells. Prior to this outgrowth, however, the p27 deficient cells display marked chromosomal aberrations, including translocations and inversions, indicating a clear contribution to genetic instability.

Since p27 deficiency did not affect cell proliferation indices, we analyzed cell cycle-independent roles for p27 loss in tumor development. Thus we asked if the response of p27 deficient and wild type tumor progenitors to DNA double-strand breaks was comparable. Atm and Chk2 phosphorylation kinetics were similar in wild type and p27 deficient cells. The accumulation of gH2AX was largely equivalent in these cells as well. gThe number of phospho-histone H3 positive mitotic cells decreased in both wild type and p27 deficient cells indicating intact G2/M checkpoint activation. This finding stands in contrast to a recent study that reported disruption of the G2/M checkpoint by loss of p27 in a colon cancer model (Payne et al., 2008). However, p27 deficiency increases the proliferation index in this model. Thus, disruption of the G2/M checkpoint reported by Payne and colleagues may actually be a cell cycle dependent function of p27.

Our data indicate that p27 deficient cultures had fewer Rad51 foci positive cells, suggesting that DNA repair is compromised. It was shown previously that cdk mediated phosphorylation of Ser3291 within the C-terminus of BRCA2 blocked Rad51 binding and interfered with Rad51 mediated homologous recombination (Esashi et al., 2005). We observed increased phosphorylation of TR2, a BRCA2 C-terminal peptide containing Ser3291, in p27 deficient lysates after γ-irradiation that could be partially accounted for by enhanced cyclin B1 associated kinase activity. Our data suggest that this process is attenuated by p27 deficiency, perhaps due to elevated cdk mediated phosphorylation of the BRCA2 C-terminus. Moreover, cells that had adapted to the checkpoint and entered mitosis did so with a greater number of chromatid breaks. Thus, our data is consistent with the notion that p27 deficiency attenuates the repair proficiency of cells, allowing for checkpoint adapted cells to progress with more unrepaired breaks and drive genetic instability. By disabling DNA repair, p27 deficiency may accelerate tumor growth during early tumorigenesis when the DNA damage response is thought to act as an anticancer barrier (Bartkova et al., 2005; Gorgoulis et al., 2005).

Data from our wild type and p27 deficient cells support a model in which cdk activity is directly linked to alterations in DNA repair. While we specifically looked at the regulation

of BRCA2, there are many other DNA repair enzymes that are regulated by cdk activity (Anantha et al., 2007; Gibbs et al., 1996; Huertas et al., 2008). Alternatively, it is also possible that p27 deficiency allows for the survival of a small number of G2 cells with DNA double strand breaks that eventually enter mitosis with increased damage to increase the pool of tumor initiating progenitors. Regardless, it is clear that p27 affects the efficiency of DSB repair in G2 cells, and this can contribute to its tumor suppressive function.

Supplementary Material

Refer to Web version on PubMed Central for supplementary material.

Acknowledgments

We thank Travis Stracker, John Petrini, Yossi Shiloh, Yuhui Liu, Nancy Yeh, Daniel Ciznadija, Dolores Hambardzumyan, Oren Becher, Elena Fomchenko, and Robert Finney, Katia Manova, Lei Zhang, Kalyani Chadalavada, Margaret Leversha, Jan Hendrix, and Diane Domingo. This research was supported by the US National Institutes of Health grant CA96582 (MR, AK, and EH), CA89563 (AK) and funds from The Golfers Against Cancer Foundation (AK). Additional support was provided by an Institutional Core Grant to Memorial Sloan-Kettering Cancer Center.

References

Anantha RW, Vassin VM, Borowiec JA. Sequential and synergistic modification of human RPA stimulates chromosomal DNA repair. J Biol Chem. 2007; 282:35910–23. [PubMed: 17928296]

Avilion AA, Nicolis SK, Pevny LH, Perez L, Vivian N, Lovell-Badge R. Multipotent cell lineages in early mouse development depend on SOX2 function. Genes Dev. 2003; 17:126–40. [PubMed: 12514105]

Aylon Y, Liefshitz B, Kupiec M. The CDK regulates repair of double-strand breaks by homologous recombination during the cell cycle. Embo J. 2004; 23:4868–75. [PubMed: 15549137]

Bartkova J, Horejsi Z, Koed K, Kramer A, Tort F, Zieger K, et al. DNA damage response as a candidate anti-cancer barrier in early human tumorigenesis. Nature. 2005; 434:864–70. [PubMed: 15829956]

Becher OJ, Hambardzumyan D, Fomchenko EI, Momota H, Mainwaring L, Bleau AM, et al. Gli activity correlates with tumor grade in platelet-derived growth factor-induced gliomas. Cancer Res. 2008; 68:2241–9. [PubMed: 18381430]

Blain SW, Scher HI, Cordon-Cardo C, Koff A. p27 as a target for cancer therapeutics. Cancer Cell. 2003; 3:111–5. [PubMed: 12620406]

Carneiro C, Jiao MS, Hu M, Shaffer D, Park M, Pandolfi PP, et al. p27 deficiency desensitizes Rb-/- cells to signals that trigger apoptosis during pituitary tumor development. Oncogene. 2003; 22:361–9. [PubMed: 12545157]

Casaccia-Bonnefil P, Tikoo R, Kiyokawa H, Friedrich V Jr. Chao MV, Koff A. Oligodendrocyte precursor differentiation is perturbed in the absence of the cyclin-dependent kinase inhibitor p27Kip1. Genes Dev. 1997; 11:2335–46. [PubMed: 9308962]

Cavalla P, Piva R, Bortolotto S, Grosso R, Cancelli I, Chio A, et al. p27/kip1 expression in oligodendrogliomas and its possible prognostic role. Acta Neuropathol (Berl). 1999; 98:629–34. [PubMed: 10603039]

Chibazakura T, McGrew SG, Cooper JA, Yoshikawa H, Roberts JM. Regulation of cyclin-dependent kinase activity during mitotic exit and maintenance of genome stability by p21, p27, and p107. Proc Natl Acad Sci U S A. 2004; 101:4465–70. [PubMed: 15070741]

Cipriano SC, Chen L, Burns KH, Koff A, Matzuk MM. Inhibin and p27 interact to regulate gonadal tumorigenesis. Mol Endocrinol. 2001; 15:985–96. [PubMed: 11376116]

Dai C, Celestino JC, Okada Y, Louis DN, Fuller GN, Holland EC. PDGF autocrine stimulation dedifferentiates cultured astrocytes and induces oligodendrogliomas and oligoastrocytomas from neural progenitors and astrocytes in vivo. Genes Dev. 2001; 15:1913–25. [PubMed: 11485986]

Di Cristofano A, De Acetis M, Koff A, Cordon-Cardo C, Pandolfi PP. Pten and p27KIP1 cooperate in prostate cancer tumor suppression in the mouse. Nat Genet. 2001; 27:222–4. [PubMed: 11175795]

Di Rocco F, Carroll RS, Zhang J, Black PM. Platelet-derived growth factor and its receptor expression in human oligodendrogliomas. Neurosurgery. 1998; 42:341–6. [PubMed: 9482185]

Doetsch F, Garcia-Verdugo JM, Alvarez-Buylla A. Cellular composition and three-dimensional organization of the subventricular germinal zone in the adult mammalian brain. J Neurosci. 1997; 17:5046–61. [PubMed: 9185542]

Doetsch F, Verdugo JM, Caille I, Alvarez-Buylla A, Chao MV, Casaccia-Bonnefil P. Lack of the cell-cycle inhibitor p27Kip1 results in selective increase of transit-amplifying cells for adult neurogenesis. J Neurosci. 2002; 22:2255–64. [PubMed: 11896165]

Durand B, Fero ML, Roberts JM, Raff MC. p27Kip1 alters the response of cells to mitogen and is part of a cell-intrinsic timer that arrests the cell cycle and initiates differentiation. Curr Biol. 1998; 8:431–40. [PubMed: 9550698]

Esashi F, Christ N, Gannon J, Liu Y, Hunt T, Jasin M, et al. CDK-dependent phosphorylation of BRCA2 as a regulatory mechanism for recombinational repair. Nature. 2005; 434:598–604. [PubMed: 15800615]

Fero ML, Randel E, Gurley KE, Roberts JM, Kemp CJ. The murine gene p27Kip1 is haplo-insufficient for tumour suppression. Nature. 1998; 396:177–80. [PubMed: 9823898]

Fero ML, Rivkin M, Tasch M, Porter P, Carow CE, Firpo E, et al. A syndrome of multiorgan hyperplasia with features of gigantism, tumorigenesis, and female sterility in p27(Kip1)-deficient mice. Cell. 1996; 85:733–44. [PubMed: 8646781]

Ferri AL, Cavallaro M, Braida D, Di Cristofano A, Canta A, Vezzani A, et al. Sox2 deficiency causes neurodegeneration and impaired neurogenesis in the adult mouse brain. Development. 2004; 131:3805–19. [PubMed: 15240551]

Foster ER, Downs JA. Histone H2A phosphorylation in DNA double-strand break repair. Febs J. 2005; 272:3231–40. [PubMed: 15978030]

Gibbs E, Pan ZQ, Niu H, Hurwitz J. Studies on the in vitro phosphorylation of HSSB-p34 and -p107 by cyclin-dependent kinases. Cyclin-substrate interactions dictate the efficiency of phosphorylation. J Biol Chem. 1996; 271:22847–54. [PubMed: 8798463]

Gorgoulis VG, Vassiliou LV, Karakaidos P, Zacharatos P, Kotsinas A, Liloglou T, et al. Activation of the DNA damage checkpoint and genomic instability in human precancerous lesions. Nature. 2005; 434:907–13. [PubMed: 15829965]

Haaf T, Golub EI, Reddy G, Radding CM, Ward DC. Nuclear foci of mammalian Rad51 recombination protein in somatic cells after DNA damage and its localization in synaptonemal complexes. Proc Natl Acad Sci U S A. 1995; 92:2298–302. [PubMed: 7892263]

Holland EC. Progenitor cells and glioma formation. Curr Opin Neurol. 2001; 14:683–8. [PubMed: 11723374]

Huertas P, Cortes-Ledesma F, Sartori AA, Aguilera A, Jackson SP. CDK targets Sae2 to control DNA-end resection and homologous recombination. Nature. 2008

Jin K, Mao XO, Batteur S, Sun Y, Greenberg DA. Induction of neuronal markers in bone marrow cells: differential effects of growth factors and patterns of intracellular expression. Exp Neurol. 2003; 184:78–89. [PubMed: 14637082]

Kamiya M, Nakazato Y. The expression of cell cycle regulatory proteins in oligodendroglial tumors. Clin Neuropathol. 2002; 21:52–65. [PubMed: 12005253]

Kiyokawa H, Kineman RD, Manova-Todorova KO, Soares VC, Hoffman ES, Ono M, et al. Enhanced growth of mice lacking the cyclin-dependent kinase inhibitor function of p27(Kip1). Cell. 1996; 85:721–32. [PubMed: 8646780]

Koff A. How to decrease p27Kip1 levels during tumor development. Cancer Cell. 2006; 9:75–6. [PubMed: 16473274]

Korshunov A, Golanov A, Sycheva R. Immunohistochemical markers for prognosis of oligodendroglial neoplasms. J Neurooncol. 2002; 58:237–53. [PubMed: 12187958]

Liu Y, Yeh N, Zhu XH, Leversha M, Cordon-Cardo C, Ghossein R, et al. Somatic cell type specific gene transfer reveals a tumor-promoting function for p21(Waf1/Cip1). Embo J. 2007; 26:4683–93. [PubMed: 17948060]

Martins CP, Berns A. Loss of p27(Kip1) but not p21(Cip1) decreases survival and synergizes with MYC in murine lymphomagenesis. Embo J. 2002; 21:3739–48. [PubMed: 12110586]

Musgrove EA, Davison EA, Ormandy CJ. Role of the CDK inhibitor p27 (Kip1) in mammary development and carcinogenesis: insights from knockout mice. J Mammary Gland Biol Neoplasia. 2004; 9:55–66. [PubMed: 15082918]

Nakayama K, Ishida N, Shirane M, Inomata A, Inoue T, Shishido N, et al. Mice lacking p27(Kip1) display increased body size, multiple organ hyperplasia, retinal dysplasia, and pituitary tumors. Cell. 1996; 85:707–20. [PubMed: 8646779]

Park MS, Rosai J, Nguyen HT, Capodieci P, Cordon-Cardo C, Koff A. p27 and Rb are on overlapping pathways suppressing tumorigenesis in mice. Proc Natl Acad Sci U S A. 1999; 96:6382–7. [PubMed: 10339596]

Payne SR, Zhang S, Tsuchiya K, Moser R, Gurley KE, Longton G, et al. p27kip1 deficiency impairs G2/M arrest in response to DNA damage, leading to an increase in genetic instability. Mol Cell Biol. 2008; 28:258–68. [PubMed: 17954563]

Porter PL, Malone KE, Heagerty PJ, Alexander GM, Gatti LA, Firpo EJ, et al. Expression of cell-cycle regulators p27Kip1 and cyclin E, alone and in combination, correlate with survival in young breast cancer patients. Nat Med. 1997; 3:222–5. [PubMed: 9018243]

Powell SN, Bindra RS. Targeting the DNA damage response for cancer therapy. DNA Repair (Amst). 2009; 8:1153–65. [PubMed: 19501553]

Raderschall E, Golub EI, Haaf T. Nuclear foci of mammalian recombination proteins are located at single-stranded DNA regions formed after DNA damage. Proc Natl Acad Sci U S A. 1999; 96:1921–6. [PubMed: 10051570]

Sarkaria JN, Busby EC, Tibbetts RS, Roos P, Taya Y, Karnitz LM, et al. Inhibition of ATM and ATR kinase activities by the radiosensitizing agent, caffeine. Cancer Res. 1999; 59:4375–82. [PubMed: 10485486]

Shaffer DR, Viale A, Ishiwata R, Leversha M, Olgac S, Manova K, et al. Evidence for a p27 tumor suppressive function independent of its role regulating cell proliferation in the prostate. Proc Natl Acad Sci U S A. 2005; 102:210–5. [PubMed: 15615849]

Sherr CJ, Roberts JM. Inhibitors of mammalian G1 cyclin-dependent kinases. Genes Dev. 1995; 9:1149–63. [PubMed: 7758941]

Sherr CJ, Roberts JM. CDK inhibitors: positive and negative regulators of G1-phase progression. Genes Dev. 1999; 13:1501–12. [PubMed: 10385618]

Shih AH, Dai C, Hu X, Rosenblum MK, Koutcher JA, Holland EC. Dose-dependent effects of platelet-derived growth factor-B on glial tumorigenesis. Cancer Res. 2004; 64:4783–9. [PubMed: 15256447]

Soos TJ, Kiyokawa H, Yan JS, Rubin MS, Giordano A, DeBlasio A, et al. Formation of p27-CDK complexes during the human mitotic cell cycle. Cell Growth Differ. 1996; 7:135–46. [PubMed: 8822197]

Spruck CH, Won KA, Reed SI. Deregulated cyclin E induces chromosome instability. Nature. 1999; 401:297–300. [PubMed: 10499591]

Strohmaier H, Spruck CH, Kaiser P, Won KA, Sangfelt O, Reed SI. Human F-box protein hCdc4 targets cyclin E for proteolysis and is mutated in a breast cancer cell line. Nature. 2001; 413:316–22. [PubMed: 11565034]

Uhrbom L, Hesselager G, Nister M, Westermark B. Induction of brain tumors in mice using a recombinant platelet-derived growth factor B-chain retrovirus. Cancer Res. 1998; 58:5275–9. [PubMed: 9850047]

Uhrbom L, Holland EC. Modeling gliomagenesis with somatic cell gene transfer using retroviral vectors. J Neurooncol. 2001; 53:297–305. [PubMed: 11718262]

Weinstock DM, Richardson CA, Elliott B, Jasin M. Modeling oncogenic translocations: distinct roles for double-strand break repair pathways in translocation formation in mammalian cells. DNA Repair (Amst). 2006; 5:1065–74. [PubMed: 16815104]

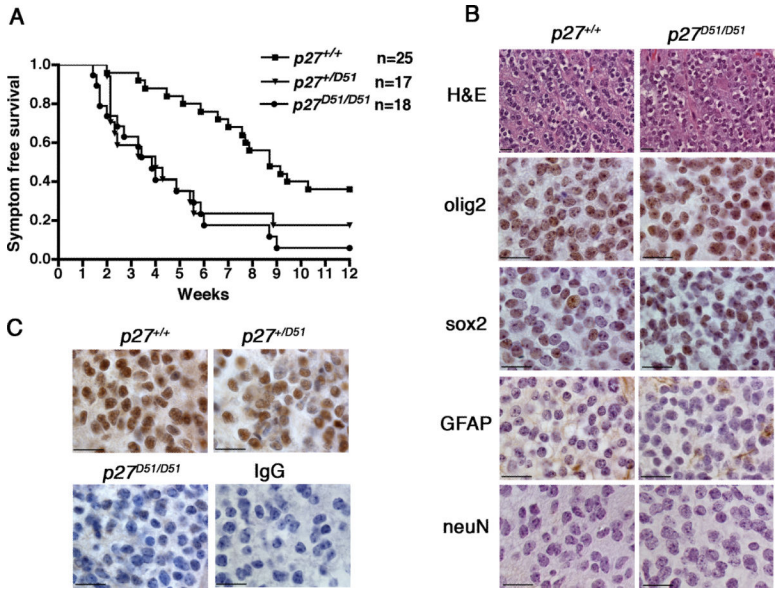

Figure 1. p27 deficiency causes a decrease in survival in PDGF-induced oligodendrogliomas

(A) Ntv-a+ neonatal mice were injected into the frontal cortex with 10^4 DF1 packaging cells expressing the RCAS-PDGF-HA virus. Mice were sacrificed at 12 weeks or earlier if symptoms presented. (log-rank analysis, $p27^{+/+}$ versus $p27^{D51/D51}$, P<0.0001; $p27^{+/+}$ versus $p27^{+/D51}$, P<0.02; $p27^{+/D51}$ versus $p27^{D51/D51}$, P<0.5) **(B)** Mouse brain sections were fixed and stained with the indicated antibodies. Bar, 20 μm. (**C**) Immunohistochemistry was performed on mouse brain tumors using p27 antibodies. Bar, 20 μm.

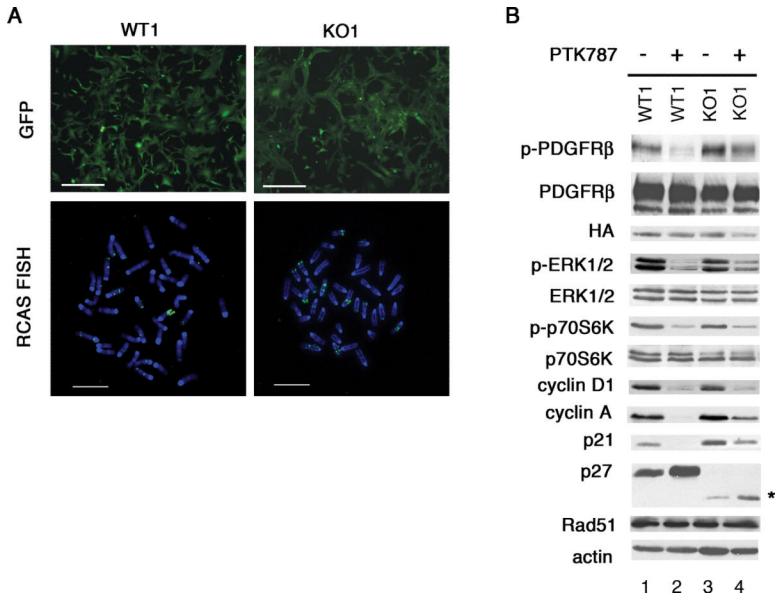

Figure 2. Wild type and p27 deficient glial cells lines were generated from primary brain cultures by infection with the RCAS/PDGF/GFP virus

(A) Wild type (WT1) and p27 deficient (KO1) brain cultures were infected with RCAS-PDGF-GFP and cultured for 6-8 weeks. Fluorescence microscopy showed that greater than 99% of RCAS-PDGF-GFP infected cells expressed GFP (upper panels). Bar, 250 μM. RCAS integration was detected by FISH (lower panels). Bar, 8 μM. **(B)** Early passage (≤p20) WT1 and KO1 cells were serum starved for 24 hours and treated with 1 μM PTK787, except for phospho-p70S6K which could only be detected in the presence of serum, and lysates were subjected to immunoblot analysis using the indicated antibodies. Rad51 was detected after 3 days of PTK787 treatment. The asterik on the right of the p27 panel indicates the band that represents the protein produced from the D51 allele.

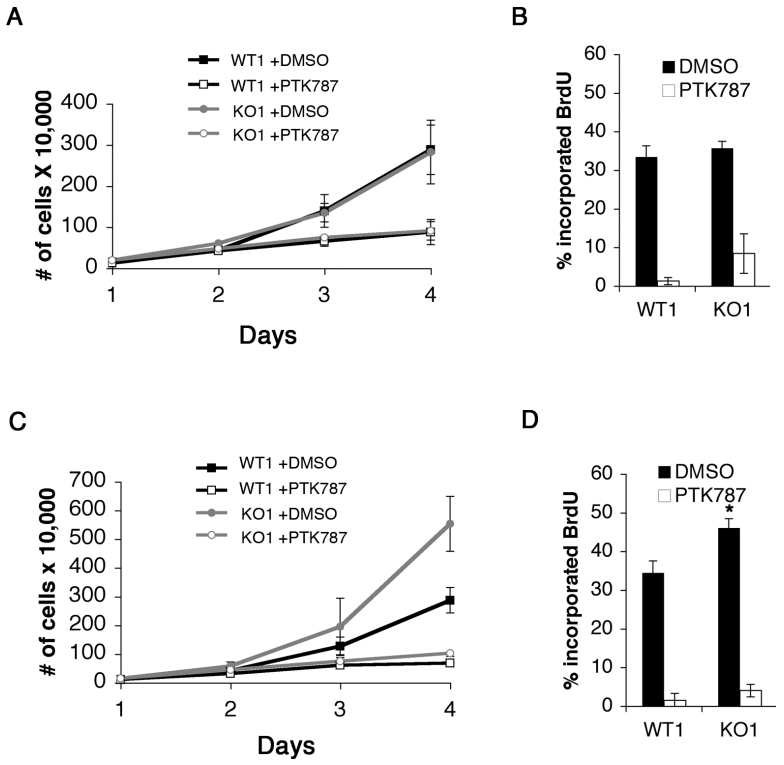

Figure 3. Wild type and p27 deficient PDGF/GFP-infected glial cell lines have similar growth and proliferation rates at early passage and are sensitive to PDGFR kinase inhibition

(A) Early passage WT1 and KO1 glial cell lines were plated at low density and treated with DMSO or 1 μM PTK787, a PDGFR kinase inhibitor. The cells were then counted every day for four days to measure cell growth. The mean and standard deviation were compiled from three independent experiments. **(B)** Early passage WT1 and KO1 cells were treated with DMSO for 24 hours or 1 μM PTK787 for three days, labeled with BrdU for one hour, and analyzed by flow cytometry. The mean and standard deviation were compiled from three independent experiments. **(C)** High passage (>p20) WT1 and KO1 glial cell lines were plated at low density and treated with DMSO or 1 μM PTK787, a PDGFR kinase inhibitor. The cells were counted every day for four days to measure cell growth. The mean and standard deviation were compiled from three independent experiments. **(D)** High passage WT1 and KO1 cells were treated with DMSO for 24 hours or PTK787 for three days, labeled with BrdU for one hour, and analyzed by flow cytometry. The mean and standard deviation were compiled from three independent experiments (WT1 versus KO1 DMSO treated, *P<0.02).

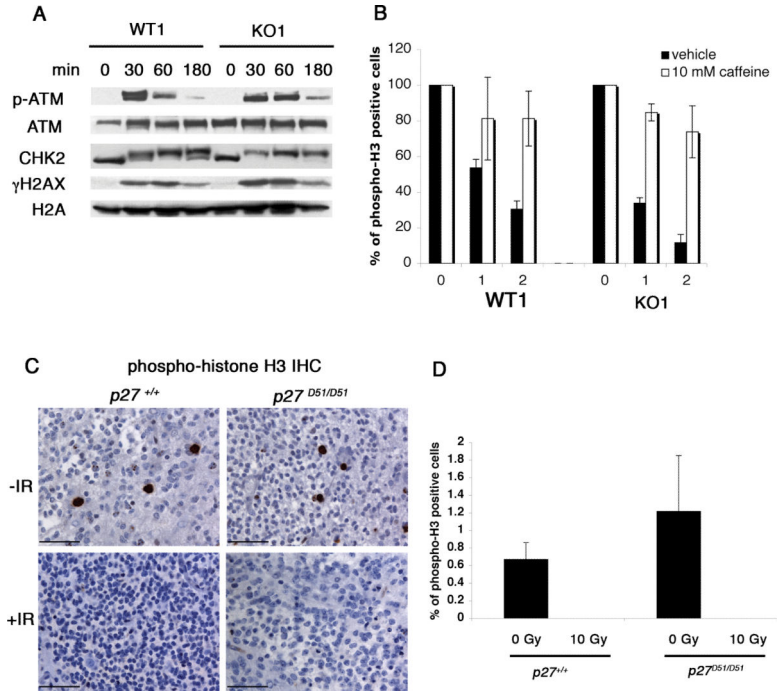

Figure 4. p27 deficient cells activate the DNA damage response and maintain the G2/M checkpoint

(A) WT1 and KO1 cells were irradiated (5 Gy) and lysed at indicated time points. Lysates were subjected to immunoblot analysis using the indicated antibodies. **(B)** WT1 and KO1 were treated with (open bars) and without (black bars) 10 mM caffeine for 30 minutes, irradiated (1 or 2 Gy), and then allowed to recover for one hour. Mitotic cells were detected by flow cytometry using propidium iodide and phospho-H3 antibodies. The mean and standard deviation was compiled from three to six independent experiments. **(C)** $p27^{+/+}$ (n=3) and $p27^{D51/D51}$ (n=2) tumor bearing mice were irradiated with 10 Gy and allowed to recover for 3 hours. Brains from irradiated and unirradiated ($p27^{+/+}$, n=3; $p27^{D51/D51}$, n=3) tumor bearing mice were fixed and stained with phospho-histone H3 antibodies. Bar, 50 μM. **(D)** Phospho-histone H3 stained tumors were imaged (three areas per tumor) and positive staining was quantified using Metamorph software. The mean and standard deviation were compiled from three independent tumors.

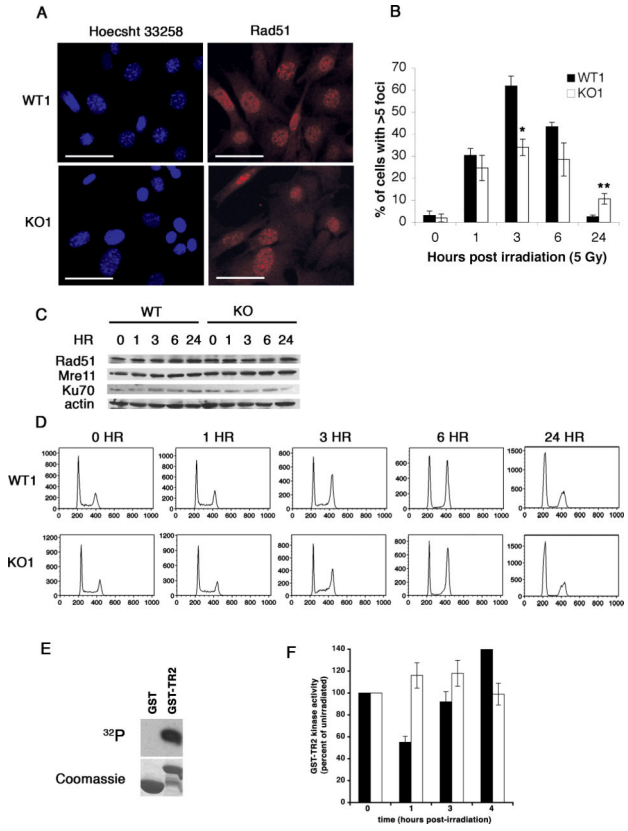

Figure 5. p27 deficient cells are defective in Rad51 nuclear foci formation and contain elevated GST-TR2 phosphorylation activity in response to γ-irradiation

(A and B) WT1 and KO1 cells were irradiated (5 Gy) and analyzed by immunofluorescence using Rad51 antibodies at 0, 1, 3, 6, and 24 hours. **(A)** Representative images three hours post-irradiation. Bar, 50 μm. **(B)** Percent of cells containing >5 Rad51 nuclear foci. The mean and standard deviation were compiled from three to six independent experiments. (WT1 versus KO1 3 hours post-irradiation, *P<0.001; WT1 versus KO1 24 hours post-irradiation, **P<0.05). **(C)** Wild type and p27 deficient cells were irradiated (5 Gy) and subjected to immunoblot analysis at the indicated time points. **(D)** Representative cell cycle profiles. Cells were irradiated (5 Gy), fixed at the indicated time points, stained with propidium iodide, and analyzed by flow cytometry. **(E and F) GST-TR2 kinase assay. (E)** GST is not phosphorylated in this assay. This is a representative autoradiogram of three independent experiments assessing the GST and GST-TR2 kinase activity in 14 mg of unirradiated lysate from wild type cells. The top panel is the autoradiogram and the bottom panel is the coomassie stained gel showing the different substrates in each lane. **(F)** WT1 (black bars) and KO1 cells (open bars) were irradiated (5 Gy) and lysed at the indicated time points. Lysates were subjected to kinase assays using GST-TR2 as a substrate. The mean and standard deviation are compiled from three independent experiments.

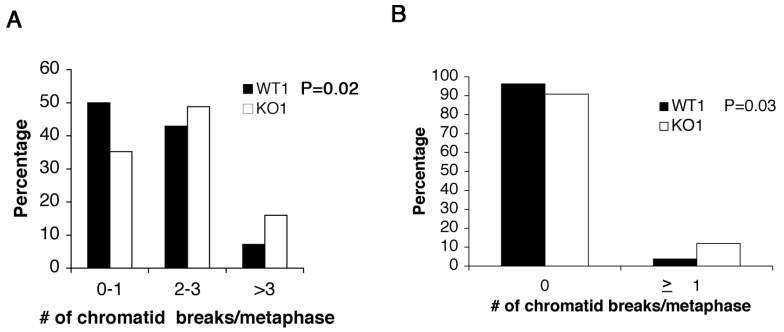

Figure 6. p27 deficient cells contain increased chromatid breaks in response to γ-irradiation

(A) WT1 and KO1 cells were irradiated (1 Gy) and cultured for 1.5 hours. Cells were then treated with colcemid for 1 hour and karyotype analysis was performed. The number of chromatid breaks was quantified (Chi-square anlaysis, WT1 versus KO1, *P=0.02). **(B)** WT1 and KO1 cells were irradiated (5 Gy) and karyotype analysis was performed 24 hours post-irradiation. The number of chromatid breaks was quantified (Chi-square anlaysis, WT1 versus KO1, *P=0.03).

Table 1

Karyotype abnormalities

Cell Line	%RCAS positive	# of abnormal cells[a]/total cells	P-value[d]
WT1	>99	3/23	
KO1	>99	24/32[b]	<0.0001
WT2	>99	5/23	
KO2	>99	18/25[c]	<0.001
Tumor			
p27 $^{+/+}$	89	5/50	
p27$^{D51/D51}$	82	31/50	<0.0001

[a] includes aneuploid and tetraploid cells

[b] fifty percent of the cells contained a translocation, t(9,18)

[c] forty percent of the cells contained an inversion, inv(17)(qAqE)

[d] P-value was calculated using Fisher's exact test

Table 2

Mitotic chromatid breaks in primary tumors

Genotype	# of cells with breaks/total cells[a]	P-value[b]
$p27^{+/+}$	5/50	
$p27^{D51/D51}$	13/50	<0.02

[a] most cells contained ≤2 breaks per cell

[b] P-value was calculated using Fisher's exact test